Proceedings of International Collaboration on Advanced Neutron Sources (ICANS-VII), 1983 September 13-16
Atomic Energy of Canada Limited, Report AECL-8488

VALIDATION OF SPALLATION MODELS FOR PARTICLE PRODUCTION

D. Filges, T.W. Armstrong*, P. Cloth

Institut für Reaktorentwicklung, Kernforschungsanlage Jülich GmbH
Postfach 1913, D-5170 Jülich, Germany
*KFA Consultant, P.O. Box 2807, La Jolla California 92038, USA

ABSTRACT

The intranuclear-cascade-evaporation model has been used to predict the neutron production from nonelastic interactions of protons with several target materials as U, Pb, Ta, In, Nb, Fe, Al and C. These model predictions for a 590 MeV proton beam were compared with measurements of Cierjacks et al. /1/ made at the SIN facility. In general the model predicts approximately the correct neutron production in the evaporation region, whereas in the high energy region (>100 MeV) are substantially discrepancies between measurement and model predictions. As an example calculated yields for ^{3}He and ^{4}He production were also compared with measured cross sections. From these limited comparisons shown here it is evident that there are large differences between theoretical evaluations and measurements.

INTRODUCTION

As part of a study to assess the accuracy of state-of-the-art high-energy models for spallation neutron source applications, the intranuclear-cascade-evaporation model has been used to predict the double differential neutron production cross sections for nonelastic collisions of protons with uranium, lead, tantalum, indium, niobium, iron, aluminium and carbon nuclei. The purpose here is to predict some comparisons of model validation calculations mainly with experimental data for neutron spectra produced in thin targets.

CALCULATIONAL PROCEDURE

The calculations are made using HETC/KFA-1 /2/ with the so- called "thin target setup" with 590 MeV protons. For uranium the Rutherford and Appleton high energy fission model (RAL) /2/ with B_0 = 8 MeV and the production of secondary evaporation particles isotropically in the lab system were used /2/. For all other targets the variable B_0-option of HETC/KFA-1, without high energy fission and a non isotropic emission for evaporation was assumed.

All cases were run with about 30000 real collisions per target with 1 hour computer time on IBM-3033. The cases were measured by S. Cierjacks et al. /1/ and the final evaluation of the measured data for materials U, Pb, Ta, In, Nb, Fe, Al and C measured at angles of 30°, 90° and 150° were compared. The materials input for HETC/KFA-1 is given in Table I and the energy and angle grids for the analysis is shown in Table II.

Table I Material Input

Target	Z	A	N_A(Atoms/cm^3 x 10^{-24})
U	92	238	0.0483
Pb	82	207	0.0329
Ta	73	181	0.0552
In	49	115	0.0382
Nb	41	93	0.0554
Fe	26	56	0.0846
Al	13	27	0.0602
C	6	12	0.1104

Table II Energy and Angle Grid for Analysis of HETC/KFA-1 Results

Energy Grid		θ Grid
0	15	0°
0.15	20	5
0.2	30	10
0.3	40	15
0.4	60	20
0.6	80	25
0.8	100	35
1.0	150	40
1.5	200	50
2.0	300	65
3.0	400	80
4.0	500	100
6.0	600	120
8.0		140
10.0		160
		180
27 ΔE Intervals		15 ΔE Intervals

For evaporation particles the following angle grid is used

Calculated Evap.	Angle in Experiment
0° - 60°	23° / 30°
60° - 120°	90°
120° - 150°	150°

The following results were evaluated from the HETC/KFA-1 calculations

double-differential yield spectra for each particle type

Y_i (E,θ), no./(MeV.str) per incident proton

where i= emitted particle type
= n(evap+cascade), p(evap+cascade), d, t, ^{3}He, α, π^+, π^0, π^-.

- marginal distributions, summed over angle:

Y_i (E), no./MeV per proton

- marginal distributions, summed over energy:

  $Y_i(\theta)$, no./str. per proton

- total yield, over all energy and angle:

  Y_i, no. per proton

To compare with the KfK data in terms of cross sections, the "yield spectra" must be multiplied by the inelastic cross section σ_{in}, computed by HETC, which can be obtained in the following way:

From HETC listing (printed information at beginning of run) the value for the macroscopic geometric cross section, Σ, is printed (in units of cm^{-1}).

Then, in units of barns:

$$\sigma_{in} = \Sigma_{in}/N_a = 1/N_a \times \Sigma_G \times F_R$$

where N_a = atom density value used in HETC input

F_R = fraction of incident protons that have "real" collisions

$$= \frac{\text{(no. real collisions)}}{\text{(no.real collisions + no.pseudo collisions)}}$$

where these are values printed at end of HETC output.

Then

$$d^2\sigma/dE d\Omega \quad (b/MeV.str) = Y_n(E,\theta)\ \sigma_{in}$$

is to be compared with KfK data.
In Table III the calculated σ_{in} vs. A number are given.

Table III Calculated σ_{in} vs. A number

Mass Number A	σ_{in} (barn)
U-238	1.849
Pb-207	1.683
Ta-181	1.563
In-115	1.183
Nb-93	1.035
Fe-56	0.7486
Al-27	0.4622
C-12	0.2629

NEUTRON SPECTRA COMPARISONS

We show only some examples of the whole comparisons which are made. The complete validation is given in Ref. /3/. Figures 1-4 show comparisons of the calculations and KfK measurements for neutron spectra of uranium at 30°, 90° and 150°, Figures 5-8 for lead, Figures 9-12 for iron and Figures 13-16 for carbon. The basic conclusions we draw from these comparisons are: (a) for all materials there is a good agreement in the evaporation region of the spectrum (few MeV upto 20 MeV) except for the lighter materials as Al and C. The high energy part of the spectrum (> 100 MeV) is underestimated by the calculations, by a factor of 2-3 for small (e.g. 30°) angles, with much worse agreement at the higher angles. This is similar for all target materials.

GAS PRODUCTION CROSS SECTIONS

Also low energy charged particle production from nuclear collisions is very important for predictions related to radiation effects and material selection for high current spallation facilities /4/,/5/. The used nuclear models /2/ are capable of calculating the spatial dependent production of low-energy particles as H, d, t, ^{3}He and ^{4}He. But very little was done to check evaluations against experiments. Together with our evaluation of neutron production measurements of Cierjacks et al. /1/ we got HETC/KFA-1 calculated low energy charged particle cross sections. We compared this data with several sets of measurements which have been made for various target materials for proton beam of about 600 MeV.

As an example in Fig. 17 and 18 the calculated ^{3}He and ^{4}He production cross section vs. A are compared with measured cross sections. The measured data are from several different experiments at, or near, 600 MeV mainly from Ref. /6/. From the limited comparisons shown here it is evident that there are large differences between theoretical evaluations and measurements.

CONCLUSIONS

The major deficiency of the present model is considered to be the underestimate of the high-energy neutrons and protons. We predict the correct neutron production in the evaporation region for elements heavier than iron with larger differences for lighter elements. The present comparisons show an underestimation at high energies (> 100 MeV) by a factor of 2-3 for small angles (e.g. 30°), with much worse agreement at higher angles 90° and 150°. The magnitude of the difference is still questionable because of the energy resolution due to the very short flight pathes (∿1 m length). There are model changes which would, we believe, improve the high-energy particle production. But measurements at other energies and with better resolution are needed to provide a complete evaluation.

For that purpose model validation experiments (KFA-LANL(P9)-Collaboration are underway. In the meantime, this problem must be kept in mind in making predictions related to SNQ design.

REFERENCES

/1/ S. Cierjacks, Y. Hino, S.D. Howe, F. Roupp, L. Buth
Differential Neutron Production Cross Section for 590 Protons, Proceedings of the Interna- tional Conference "Nuclear Data for Science and Technology" 6-10 September 1982, Antwerp

/2/ P. Cloth, D. Filges, G. Sterzenbach, T.W. Armstrong, B.L. Colborn
The KFA-Version of the High-Energy Transport Code HETC and the generalized Evaluation Code SIMPEL, KFA-Report, Jül-Spez-196, March 1983

/3/ To be published

/4/ W. Lohmann
Materials Problems in Beam Windows and Structural Components of the SNQ-Target, Proc. 4th Meeting of the International Collaboration on Advanced Neutron Sources (ICANS-IV), Tsukuba, Japan, October 20-24, 1980 (KENS Report II, March, 1981)

/5/ J. Jung
Radiation Effects in Target and Structural Components of a Spallation Neutron Source, Proc. 5th Meeting of the International Collaboration on Advanced Neutron Sources (ICANS-IV) G.S. Bauer and D. Filges (Eds.) Jülich, FRG, June 22-26, 1981 (Jül-Conf-45, Oct. 1981)

/6/ S.T. Kruger, D. Heymann
High-Energy Proton Production of ^{3}H, ^{3}He, and ^{4}He in Light Targets, Phys. Rev. C 7, 2179 (1973)

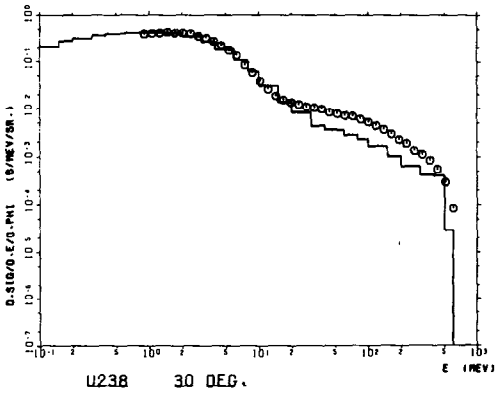

Figure 1 Comparison of calculated and KfK measured neutron cross sections at 30° from a thin uranium target bombarded by 590 MeV protons

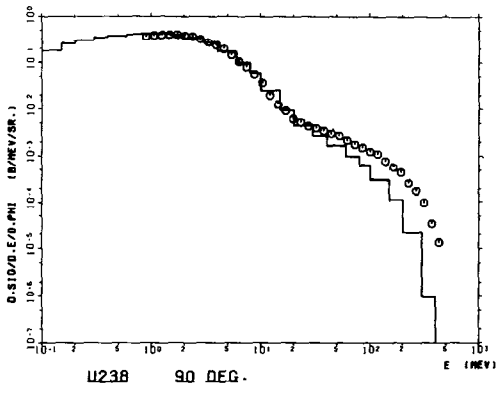

Figure 2 Comparison of calculated and KfK measured neutron cross sections at 90° from a thin uranium target bombarded by 590 MeV protons

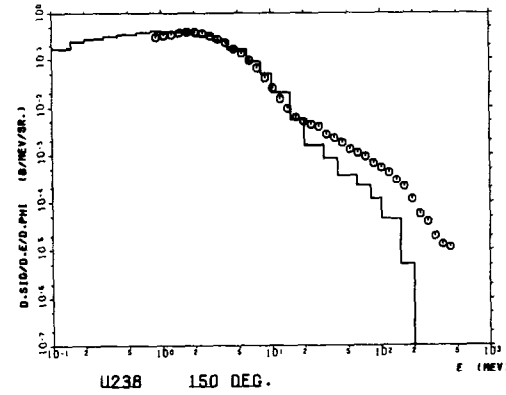

Figure 3 Comparison of calculated and KfK measured neutron cross sections at 150° from a thin uranium target bombarded by 590 MeV protons

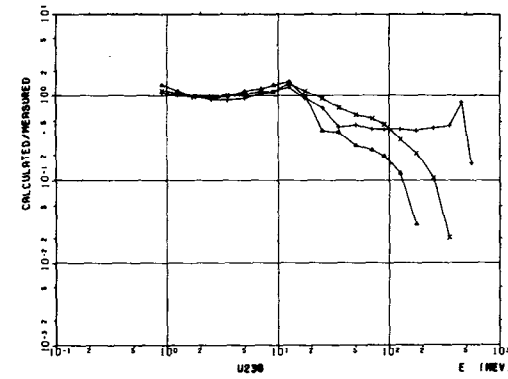

Figure 4 Ratio of calculated to measured neutron cross sections from a thin uranium target bombarded by 590 MeV protons

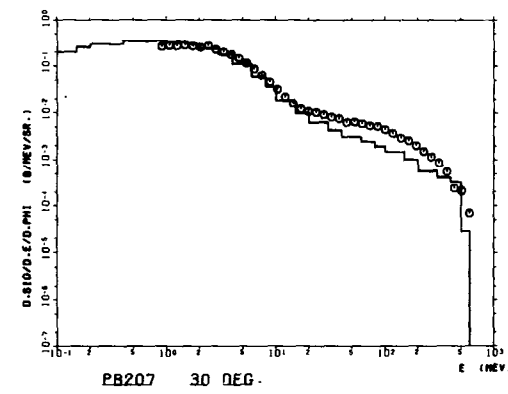

Figure 5 Comparison of calculated and KfK measured neutron cross sections at 30° from a thin lead target bombarded by 590 MeV protons

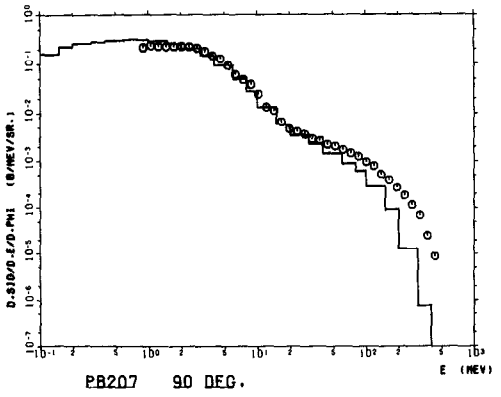

Figure 6 Comparison of calculated and KfK measured neutron cross sections at 90° from a thin lead target bombarded by 590 MeV protons

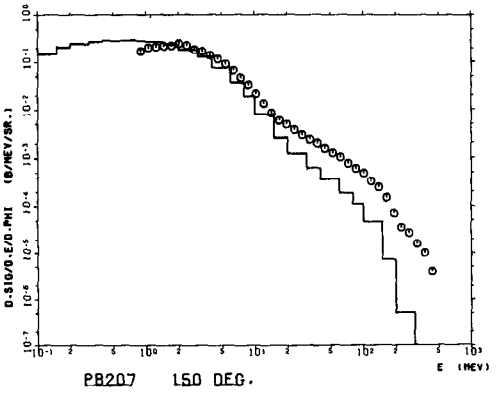

Figure 7 Comparison of calculated and KfK measured neutron cross sections at 150° from a thin lead target bombarded by 590 MeV protons

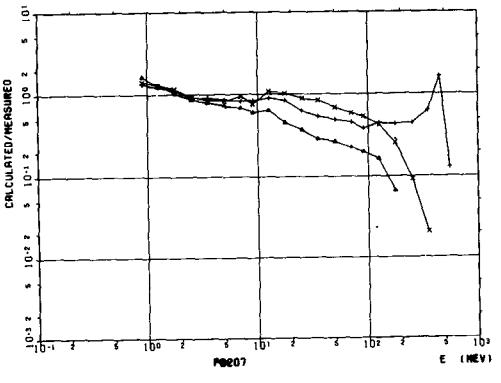

Figure 8 Ratio of calculated to measured neutron cross sections from a thin lead target bombarded by 590 MeV protons

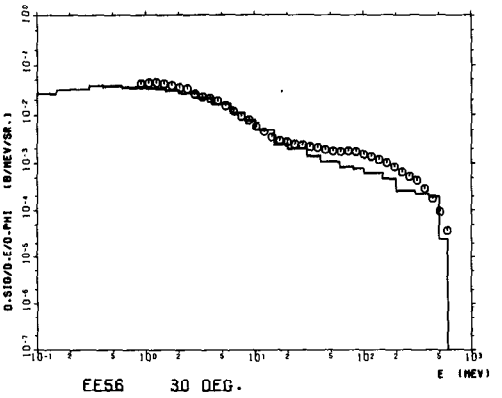

Figure 9 Comparison of calculated and KfK measured neutron cross sections at 30° from a thin iron target bombarded by 590 MeV protons

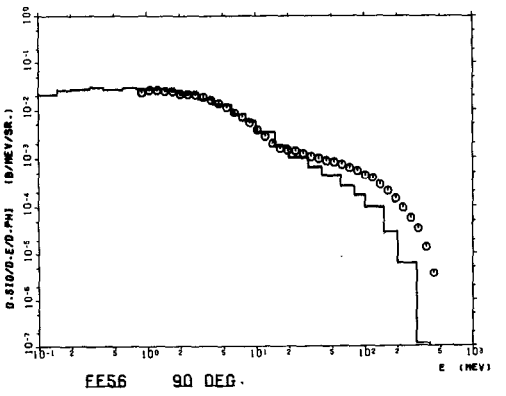

Figure 10 Comparison of calculated and KfK measured neutron cross sections at 90° from a thin iron target bombarded by 590 MeV protons

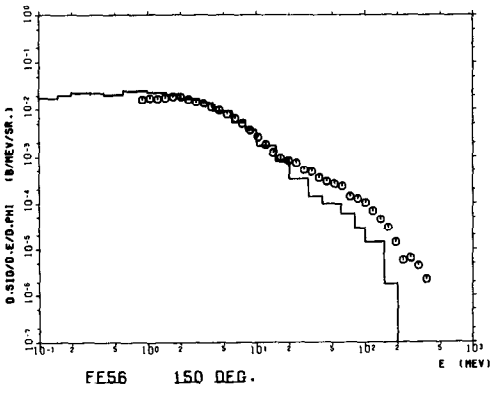

Figure 11 Comparison of calculated and KfK measured neutron cross sections at 150° from a thin iron target bombarded by 590 MeV protons

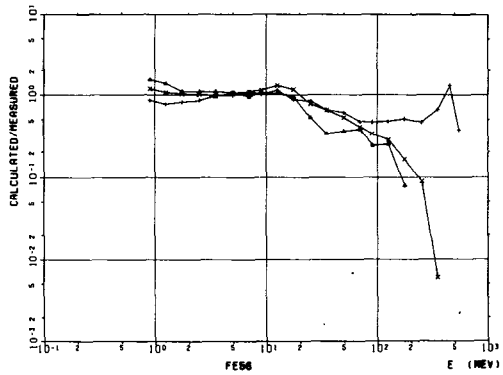

Figure 12 Ratio of calculated to measured neutron cross sections from a thin iron target bombarded by 590 MeV protons

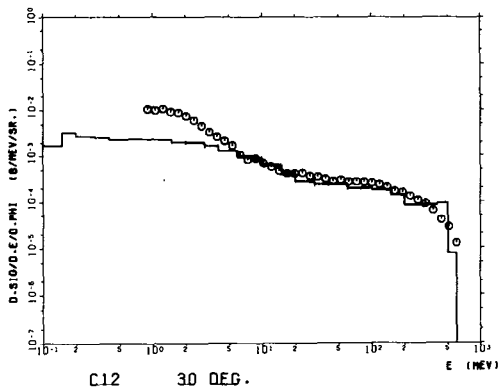

Figure 13 Comparison of calculated and KfK measured neutron cross sections at 30° from a thin carbon target bombarded by 590 MeV protons

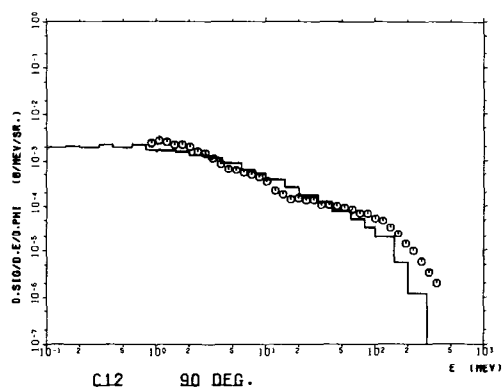

Figure 14 Comparison of calculated and KfK measured neutron cross sections at 90° from a thin carbon target bombarded by 590 MeV protons

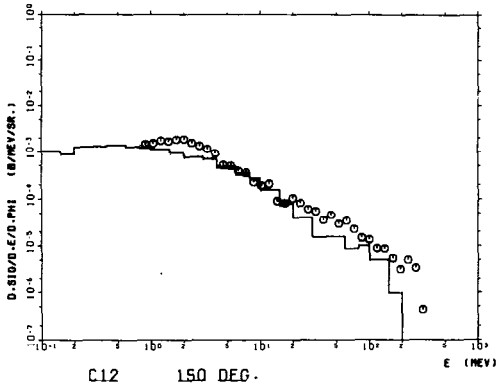

Figure 15 Comparison of calculated and KfK measured neutron cross sections at 150° from a thin carbon target bombarded by 590 MeV protons

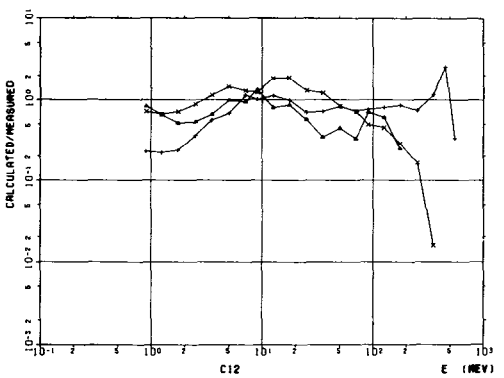

Figure 16 Ratio of calculated to measured neutron cross sections from a thin carbon target bombarded by 590 MeV protons

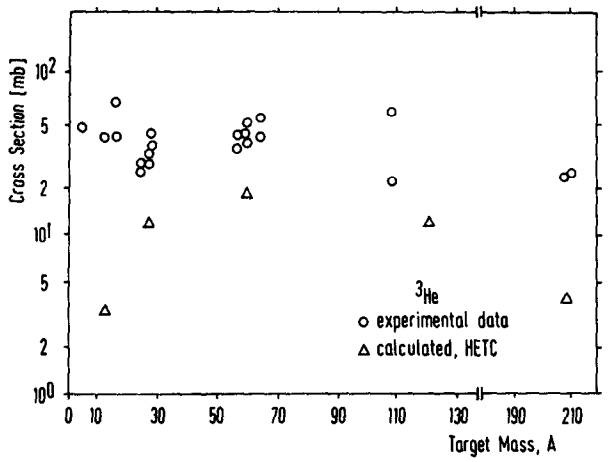

Figure 17 Comparison of HETC calculated cross sections for ^{3}He production with experimental data /6/ for 600 MeV proton bombardment

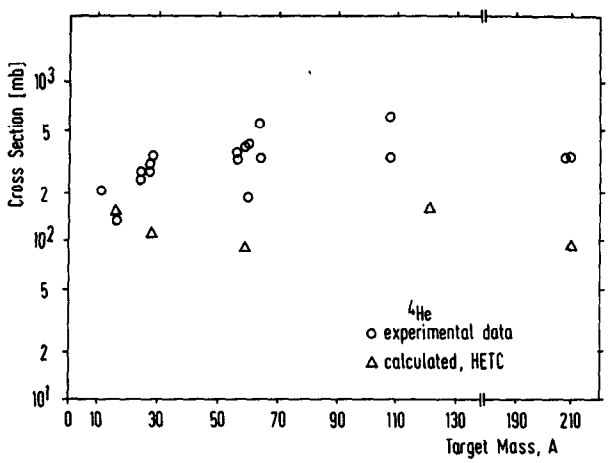

Figure 18 Comparison of HETC calculated cross sections for ^{4}He production with experimental data /6/ for 600 MeV proton bombardment